Electron. Mater. Lett., Vol. 13, No. 2 (2017), pp. 129-135
DOI: 10.1007/s13391-017-6164-z

Gd Doping Effect on Structural, Electrical and Magnetic Properties of ZnO Thin Films Synthesized by Sol-Gel Spin Coating Technique

Sanjeev Kumar[1,*] and Rajalingam Thangavel[2]

[1]Department of Applied Sciences, PEC University of Technology, Chandigarh 160012, India
[2]Department of Applied Physics, Indian Institute of Technology (Indian School of Mines), Dhanbad 826004, India

(received date: 1 June 2016 / accepted date: 3 December 2016 / published date: 10 March 2017)

Nanocrystalline Gd-doped ZnO thin films were deposited on sapphire (0001) substrates using sol-gel spin coating technique. The structural and optical properties of deposited thin films were characterized by X-ray diffraction (XRD) and micro Raman spectroscopy. Structural and optical studies show that the doped Gd ions occupy Zn sites retaining the wurtzite symmetry. Photoluminescence (PL) studies reveal the presence of oxygen vacancies in Gd doped ZnO thin films. The resistivity of Gd doped ZnO thin film decreases with increase in Gd doping upto 4%. Gd-doped ZnO films demonstrate weak magnetic ordering at room temperature.

Keywords: X-ray diffraction, electron microscopy, raman scattering, photoluminescence, ferromagnetism

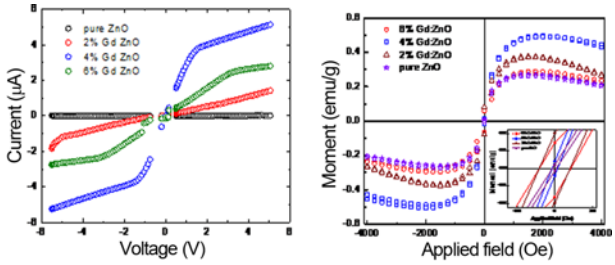

1. INTRODUCTION

The magnetic semiconductors have fascinated the field of spintronics which together exploits the charge and spin of electrons.[1] The appropriateness of dilute magnetic semiconductors (DMSs) for spintronics applications is resulting from its capability to dope a small part of host semiconductor cations with magnetic ions.[2] Theoretical calculations proposed that the wide band-gap semiconductors doped with a competent transition metals, escort to the development of the room temperature ferromagnetism (RTFM).[3] Usually, the 3*d* electrons in transition metals are delocalized and exterior, escorting to strong direct exchange interactions. But in case of, rare earth metals, the 4*f* electrons, are localized and leading to indirect exchange interactions resulting in high magnetic moments per atom.[4] ZnO is a wide-gap semiconductor (3.37 eV) having large exciton binding energy of 60 meV at room temperature. Magnetic properties of transition metal doped ZnO has been broadly investigated experimentally[5,6] as well as theoretically.[3]

Potzger *et al.*[7] reported ferromagnetism in Gd-implanted ZnO single crystals. They also reported that there should be a sufficient density of Gd ions and annealing is also required to release enough charge carriers resulting in ferromagnetism in Gd implanted ZnO single crystals. Ney *et al.*[8] reported that the Gd-implanted ZnO shows RTFM and the FM increases with low temperature high vacuum annealing. They also reported that the origin of the ferromagnetism appears to be electron mediated. Shi *et al.*[9] theoretically concluded that the electrons can mediate the ferromagnetism in the Gd doped ZnO system due to the *s-f* coupling between the Gd ions, *f*, and the host, *s*, states. They also suggested that the appropriate concentration of electrons should be there in order to achieve RTFM in the thin films.

Subramanian *et al.*[2] has reported intrinsic ferromagnetism and magnetic anisotropy in Gd-doped ZnO thin films synthesized by pulsed spray pyrolysis method. They suggested that Gd is doped in +3 state in host ZnO lattice

*Corresponding author: sanjeev@pec.ac.in

which increases charge carrier density. Roqan *et al.*[10] has reported the reproducible long range ferromagnetic ordering in Gd doped ZnO thin films grown using pulsed laser deposition technique. They also theoretically confirmed that Gd dopant assists in stabilizing the RTFM in Gd doped ZnO thin films.

Among various synthesis techniques, the sol-gel technique has been widely used for film deposition.[11-19] Sol-gel method allows the mixing of the chemicals at the atomic level, thus the chance of forming an untraceable impurity phase could be reduced. It shows advantages in fabricating thin homogeneous, transparent and multi-component oxide layers with many structures on various substrates.[12] Spin coating method has been used extensively for the preparation of binary and ternary oxides. It has advantages over the conventional techniques in respect of simplicity, cost effectiveness, broad range of applicability and low temperature development of thin films of oxides with low particle size.[11-19] Different groups reported the sol-gel synthesized transition metal doped dilute magnetic semiconducting thin films.[13-19]

In this paper, we report the synthesis of nanocrystalline Gd-doped ZnO thin films on sapphire substrates using sol-gel spin coating technique and their systematic characterization.

2. EXPERIMENTAL PROCEDURE

Gd doped ZnO thin films were synthesized by sol-gel spin coating technique. Zinc acetate dihydrate, gadolinium nitrate, 2-methoxyethanol and monoethanolamine (All chemicals were purchased from Sigma Aldrich) were used as the starting materials, solvent and stabilizer, respectively. Zinc acetate dihydrate and gadolinium nitrate were first dissolved in 2-methoxyethanol. The molar ratios of monoethanolamine to zinc acetate dihydrate were maintained at 1. Then, the resulting mixture was stirred at 60 °C for 2 hrs. When the mixture was stirred, monoethanolamine was added drop by drop. Finally, a clear and transparent homogeneous solution was formed. The total concentration of the solution was kept at 0.5 mol/L and the concentration of Gd dopant was 2, 4 and 6 mol% with respect to zinc. The sol was aged for 24 hours at room temperature. The sapphire substrates were cleaned in Piranha solution (H_2SO_4:H_2O_2 - 3:1), acetone and methanol for every 20 min by using ultrasonic cleaner and then cleaned with deionized water and dried under N_2 gas. The cleaned sapphire was kept at 120 °C for 5 min and the coating solution was dropped onto the sapphire substrate, which was rotated at 3000 rpm for 30 s by using a spin coater. After spin coating, the film was dried at 300 °C for 10 min on a hot plate to evaporate the solvent and to remove the organic residuals. The procedure from coating to drying was repeated ten times. The grown film was then kept in a furnace and annealed at 500 °C for 1 h.

X-ray diffraction (XRD-PANalytical) studies of the films were performed using monochromatic Cu $K\alpha_1$ radiation. The μ-PL and Resonant Raman measurements were also performed on the JobinYvon LabRAM HR 800UV micro-Raman system at room temperature, using the 325 nm line of a He-Cd laser (25 mW) as the excitation source, respectively. The number of grating grooves in the Raman spectrometer was 2400 grooves/mm for the UV laser and the laser excitation power was kept low enough to minimize sample heating which could result in thermal-induced Raman peak red shift. All Raman spectra of the ZnO films were recorded in the z (x, x) z backscattering configuration, where the z-coordinate is normal to the sample surface. Thus the polarization of the incident light was parallel to the sample surface. A 500 μm confocal pinhole was used to obtain high-resolution Raman spectra. Keithley sourcemeter (2450 Model) was used for measuring I-V characteristics of Gd doped ZnO thin films. Vibrating sample magnetometer (VSM, Quantum Design) was used for magnetic measurements at room temperature.

3. RESULTS AND DISCUSSION

Figure 1 shows the XRD patterns of spin coated undoped and Gd doped ZnO thin films on sapphire substrate. It is clearly depicted from Fig. 1 that the undoped and Gd doped ZnO thin films show only one peak corresponding to (002) plane. This diffraction peak matches with the hexagonal wurtzite ZnO structure (JCPDS No. 36 1451). Only one peak corresponding to (002) plane in the pure and Gd doped ZnO thin films indicates that the film is highly oriented along the *c*-axis. With the increase in Gd doping concentration, minor decrease in the intensity of the (002) peak depicted the minor decrease in *c*-axis oriented crystallinity (inset of

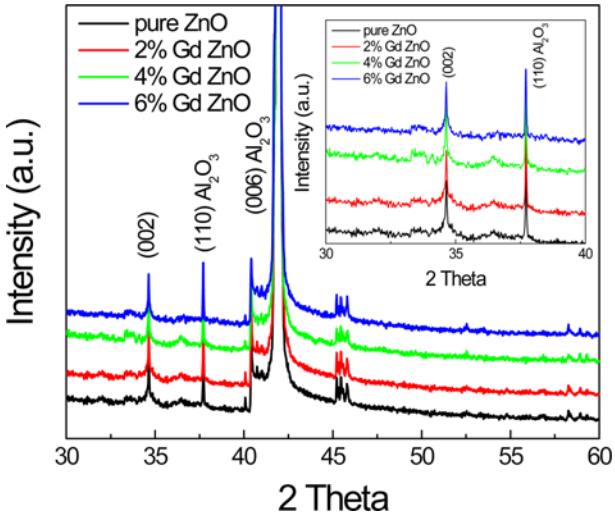

Fig. 1. XRD patterns for pure and Gd doped ZnO thin film samples deposited on sapphire substrate using sol-gel spin coating technique.

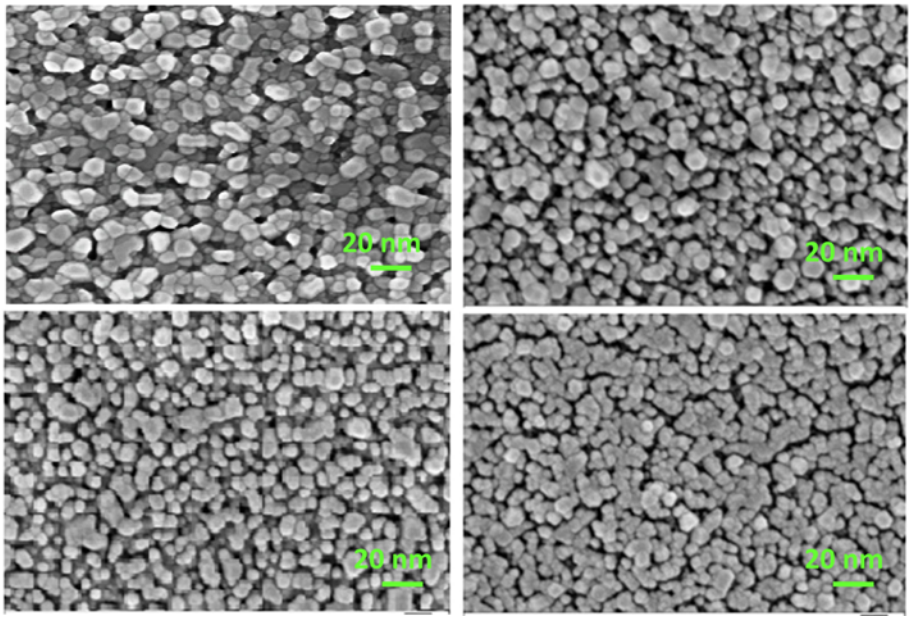

Fig. 2. SEM micrographs (top view) for pure and Gd doped ZnO thin film samples deposited on sapphire substrate using sol-gel spin coating technique

Fig. 1). No peaks related to either Gd or any of its oxides are observed in the XRD patterns, which depict that there is no extra phase present in Gd doped ZnO films. Strong peaks corresponding to sapphire substrate are also observed.

Using the diffraction peak position of (002) plane, *c*-axis length was calculated from the XRD measurement by the equation $c = (\lambda/\sin\theta)$, λ is the wavelength and θ is the Bragg diffraction angle in degrees.[20] The calculated values of the c-axis lengths were 5.210 Å, 5.199 Å, 5.186 Å, and 5.182 Å for Gd (0%, 2%, 4% and 6%) doped ZnO thin films, respectively, which leaned to minor decrease. This may be attributed due to the substitution of Gd^{3+} ions in the ZnO wurtzite host matrix. The decrease in the *c*-axis length may be due to the cationic vacancies created by Gd^{3+} doping in the ZnO host matrix. Analogous c-axis variations were also reported in Er doped ZnO,[21] Nd doped ZnO[22] and Ce doped ZnO samples.[23] Tensile stress and structural defects in the host lattice may also be induced due to the decrease in the lattice parameter in the Gd doped ZnO films.

The film surface has been investigated through SEM as shown in Fig. 2(a)-(d) and it is observed that the surface morphology of the Gd doped ZnO thin films exhibit rounded grains and connected network-like structure. The network-like structure can be attributed to the characteristic of sol-gel films. With increase in the Gd concentration the excess atoms are aggregated on the grain boundaries due to low solubility of Gd atoms in ZnO.

Figure 3 shows that the room temperature PL spectra of sol-gel spin coated Gd doped ZnO films. A strong UV emission at 377 nm, 377.5 nm, 378 nm and 380 nm is

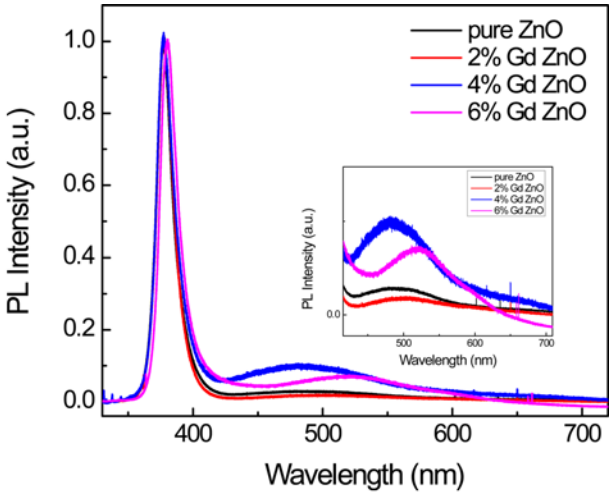

Fig. 3. Room temperature PL spectra of pure and Gd doped ZnO thin film samples deposited on sapphire substrate using sol-gel spin coating technique. Inset is showing magnified view of defect related PL spectra.

observed for undoped, 2%, 4% and 6% Gd doped ZnO thin films, respectively indicates small decrease in band-gap with an increase in Gd doping. This tunability of band-gap with Gd doping, increases the suitability of these materials for nano-optoelectronic devices. The observed PL behavior suggests that the Gd atoms get incorporated into ZnO lattice and modify the luminescence behavior. A broad peak centered at 480 nm (inset of Fig. 3) observed for undoped, 2% and 4% Gd doped ZnO thin film which is attributed to

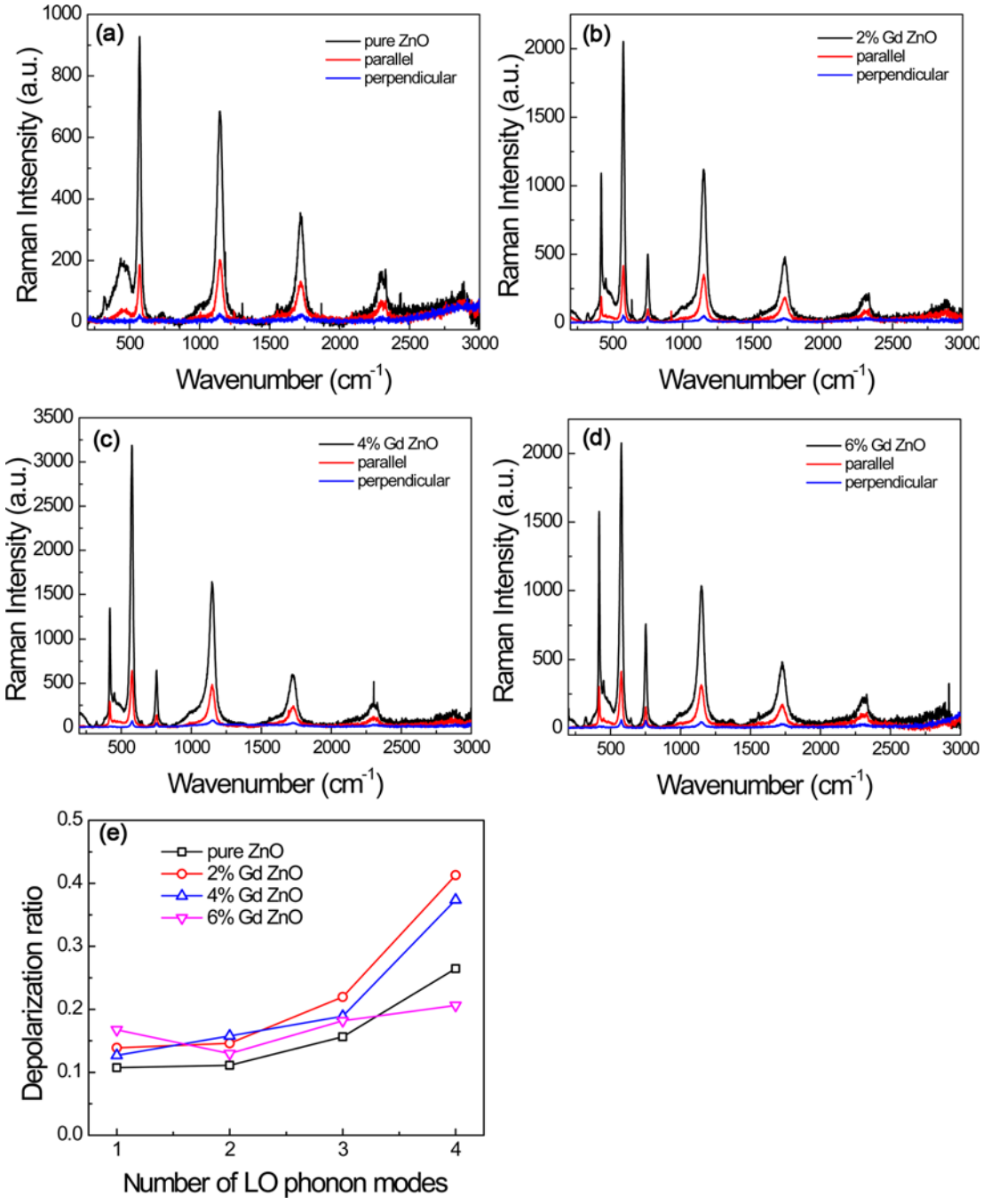

Fig. 4. (a)-(d) Room temperature Raman spectra for pure and Gd doped ZnO thin film samples deposited on sapphire substrate using sol-gel spin coating technique, (e) Variation of depolarization ratio with number of LO phonon modes for Gd doped ZnO thin film samples deposited on sapphire substrate using sol-gel spin coating technique.

oxygen vacancies.[24-26] These oxygen vacancies are also favoring the ferromagnetic ordering. A broad peak centered at 550 nm observed in 6% Gd doped ZnO thin film which is attributed to oxygen interstitials.[27]

Figure 4(a)-(d) shows the micro Raman spectra of undoped, 2%, 4% and 6% Gd doped ZnO thin films, respectively. Raman active modes observed at 321 cm^{-1}, 434 cm^{-1}, 571 cm^{-1}, 1139 cm^{-1}, 1710 cm^{-1} and 2279 cm^{-1} attributed to E_2 high-E_2 low, E_2 (high), 1st order A_1 (LO), 2nd order A_1 (LO), 3rd A_1 (LO) and 4th order A_1 (LO), respectively.[28] The peak at about 448 cm^{-1} is assigned to the high frequency branch of the E_2 (high) mode of ZnO, which is a Raman active mode in the wurtzite crystal structure and indicates that the wurtzite symmetry remain

maintained with Gd doping upto 6%.[29] As compared to pure ZnO, with the increase in Gd doping, the peak position of the E_2 (high) mode shifts to 434 cm^{-1}. Gd doping induced stress in the wurtzite ZnO structure and affects the E_2 phonon frequency.[30] An increase in the E_2 phonon frequency is credited to compressive stress, whereas a decrease in the E_2 phonon frequency is credited to a tensile stress. It is usually assumed that this stress occurs from a disparity in the thermal expansion coefficients of the nanoparticles and the substrates, or the lattice mismatch and distortion. Doping is thus considered to be the major aspect that would cause the lattice distortion of the crystals and is different due to the atomic radii of different elements.

Polarized Raman studies were performed on Gd doped ZnO thin films, with the incident light (i) parallel and (ii) perpendicular to the films and the spectra recorded under different Gd concentration are shown in Fig. 4(a)-(d), respectively. In the Polarized Raman spectra, there are no Raman modes at 275 cm^{-1}, indicating the absence of randomly distributed point defects. Strong Raman peaks at 438 and 571 cm^{-1} were observed in all the samples and were assigned to the non-polar E_2 vibration modes related to the wurtzite phase. The absence of an E_1 mode in samples depicts the development of preferred c-axis orientation in Gd doped ZnO thin films. These results corroborate with the XRD results.[31,32]

Polarized Raman spectroscopy (PRS) is used to characterize the symmetry of Gd doped ZnO films. The depolarization ratio (ρ) for a LO phonon mode is given by

$$\rho = \frac{I_{perpendicular}}{I_{parallel}}$$

where $I_{perpendicular}$ is the integrated intensity ratio of the Raman band with the polarization perpendicular to the laser beam, and $I_{parallel}$ is the integrated intensity ratio with polarization parallel to the laser beam. If $\rho < 0.75$, the vibration can be considered to be polarized, and is totally symmetric in nature. If $\rho = 0.75$, then the vibration can be considered to be depolarized, and is non-symmetric in nature.[33] From Fig. 4(e) it is clearly depicted that the depolarization ratio of *p*-type ZnO film is found to be < 0.75 and hence the symmetric nature is preserved for different Gd doping concentrations in ZnO.

Electrical characteristics of Gd doped ZnO thin films were measured under room temperature in the range of −5 to 5 V (Fig. 5). The undoped ZnO thin film exhibited the highest resistivity, while both 4% and 6% Gd doped ZnO thin film shows non-linear behavior. 4% Gd doped ZnO thin film shows highest conductivity as compared to undoped, 2% and 6% Gd doped ZnO thin film. The ionic radius of Zn^{2+} (72 pm) being significantly smaller than Gd^{3+} (94 pm), the substitution of Gd in the ZnO modifies the lattice parameters. The valence of Gd being higher than Zn, acts as a donor and

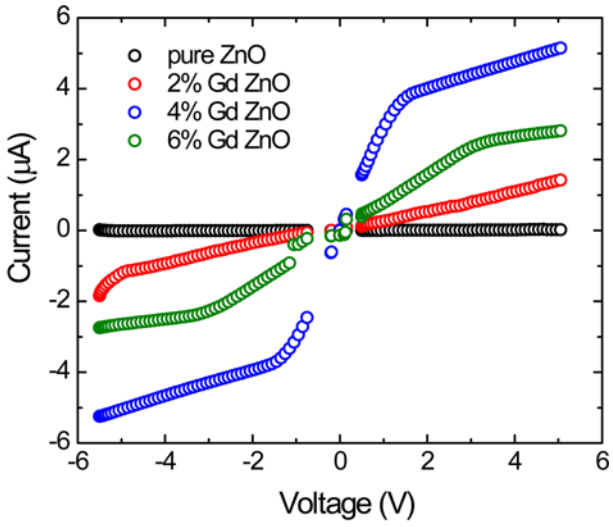

Fig. 5. Room temperature I-V characteristics for pure and Gd doped ZnO thin film samples deposited on sapphire substrate using sol-gel spin coating technique.

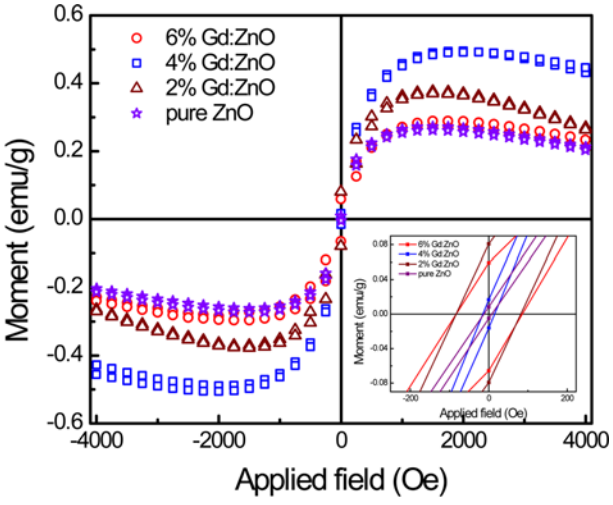

Fig. 6. Room temperature M-H curves for pure and Gd doped ZnO thin film samples deposited on sapphire substrate using sol-gel spin coating technique.

hence is expected to alter I-V characteristics. It is clearly observed from PL behavior that 4% Gd doped ZnO samples has maximum oxygen vacancies which further enhances the electrical conductivity. Undoped and 2% Gd doped ZnO thin films have less number of oxygen vacancies resulting in poor electrical conductivity. 6% Gd doped ZnO thin films have more oxygen interstitials and less oxygen vacancies depicting less conductivity in comparison to 4% Gd doped ZnO thin film.

Figure 6 presents the M-H curves for Gd doped ZnO thin films at room temperature. Pure and Gd doped ZnO thin film samples show weak ferromagnetic behavior (inset of Fig. 6).

With increase in Gd doping, magnetization increases up to 4% Gd doping. For 6% Gd doped ZnO sample again magnetization decreases. This may be due to that the Gd dopant enters into some interstitial positions in the host ZnO matrix, resulting in a decrease in Gd-Gd distance, which further results in decrease in saturation magnetization. Venkatesh *et al*.[34] also reported that oxygen deficiency related defect complexes to be responsible for ferromagnetic exchange. Similar behavior is observed in Gd doped ZnO thin films. From PL plot it is observed that peak at 480 nm corresponds to oxygen vacancies. The intensity of 480 nm peak corresponding to oxygen vacancies is maximum for 4% Gd doped ZnO sample resulting in higher magnetization and it is less for undoped, 2% and 6% Gd doped ZnO samples resulting in low magnetization.

In case of, rare earth metals, the 4*f* electrons, are confined to inner shell, which further screened by outer shell electrons. Two neighboring rare earth metal ions, due to large space between them, cannot exchange couple directly or via super-exchange interaction.[35] Ruderman-Kittel-Kasuya-Yosida (RKKY) exchange interaction is the possible one through which 4*f* and 6*s* electrons give rise to an exchange couple, which results in polarization of the *s* electrons. Spin polarized *s* electrons further influence the spin direction of the *f* electrons resulting in magnetic exchange, couples with the 4*f* electrons of the neighboring Gd ions.[35]

4. CONCLUSIONS

We have successfully grown the ZnO thin films doped with Gd on sapphire substrate using sol-gel spin coating technique. With the increase in Gd doping c-axis oriented crystallinity decreases as observed from X-ray diffraction patterns. Defects related to oxygen vacancies and oxygen interstitials are observed in PL spectra. 4% Gd doped ZnO samples shows good electrical conductivity may be due to presence of oxygen vacancies which also favors the ferromagnetic ordering in 4% Gd doped ZnO thin films. RKKY exchange interaction may be the possible exchange interaction results in ferromagnetic ordering in Gd doped ZnO thin films.

ACKNOWLEDGEMENTS

Authors are very thankful to Prof. Y.C. Chang, Research Centre for Applied Sciences, Academia Sinica, Taipei, Taiwan, for providing characterization facilities.

REFERENCES

1. P. Sharma, A. Gupta, K. V. Rao, F. J. Owens, R. Sharma, R. Ahuja, J. M. Osorio Guillen, B. Johansson, and G. A. Gehring, *Nat. Mater.* **2**, 673 (2003).
2. M. Subramanian, P. Thakur, M. Tanemura, T. Hihara, V. Ganesan, T. Soga, K. H. Chae, R. Jayavel, and T. Jimbo, *J. Appl. Phys*. **108**, 053904 (2010).
3. T. Dietl, H. Ohno, F. Matsukura, J. Cibert, and D. Ferrand, *Science* **287**, 1019 (2000).
4. G. M. Dalpian and S. H. Wei, *Phys. Rev. B* **72**, 115201 (2005).
5. M. Diaconu, H. Schmidt, H. Hochmuth, M. Lorenz, G. Benndorf, J. Lenzner, D. Spemann, D. Setzer, K. W. Nielsen, P. Esquinazi, and M. Grundmann, *Thin Solid Films* **486**, 117 (2005).
6. K. Ueda, H. Tabata, and T. Kawai, *Appl. Phys. Lett.* **79**, 988 (2001).
7. K. Potzger, S. Zhou, F. Eichhorn, M. Helm, W. Skorupa, A. Mücklich, J. Fassbender, T. Herrmannsdörfer, and A. Bianchi, *J. Appl. Phys.* **99**, 063906 (2006).
8. V. Ney, S. Ye, T. Kammermeier, A. Ney, H. Zhou, J. Fallert, H. Kalt, F. Y. Lo, A. Melnikov, and A. D. Wieck, *J. Appl. Phys*. **104**, 083904 (2008).
9. H. Shi, P. Zhang, S. S. Li, and J. B. Xia, *J. Appl. Phys.* **106**, 023910 (2009).
10. I. S. Roqan, S. Venkatesh, Z. Zhang, S. Hussain, I. Bantounas, J. B. Franklin, T. H. Flemban, B. Zou, J. S. Lee, U. Schwingenschlogl, P. K. Petrov, M. P. Ryan, and N. M. Alford, *J. Appl. Phys*. **117**, 073904 (2015).
11. G. Vijayaprasath, R. Murugan, G. Ravi, T. Mahalingam, and Y. Hayakawa, *Appl. Surf. Sci.* **313**, 870 (2014).
12. Z. G. Hu, Y. W. Li, M. Zhu, Z. Q. Zhu, and J. H. Chu, *Phys. Lett. A* **372**, 4521 (2008).
13. H. J. Lee, S. Y. Jeong, C. R. Cho, and C. H. Park, *Appl. Phys. Lett.* **81**, 4020 (2002).
14. E. Liu, P. Xiao, J. S. Chen, B. C. Lim, and L. Li, *Curr. Appl. Phys.* **8**, 408 (2008).
15. N. H. Hong, J. Sakai, and V. Brize, *J. Phys.: Condens. Matter* **19**, 036219 (2007).
16. A. Goktas, I. H. Mutlu, Y. Yamada, and E. Celik, *J. Alloy Compd.* **553**, 259 (2013).
17. J. Yang, L. Fei, H. Liu, Y. Liu, M. Gao, Y. Zhang, and L. Yang, *J. Alloy Compd.* **509**, 3672 (2011).
18. N. R. S. Farley, K. W. Edmonds, A. A. Freeman, G. van der Laan, C. R. Staddon, D. H. Gregory, and B. L. Gallagher, *New J. Phys.* **10**, 055012 (2008).
19. G. Y. Ahn, S. I. Park, S. J. Kim, B. W. Lee, and C. S. Kim, *IEEE T. Magn.* **41**, 2730 (2005).
20. B. D. Cullity, *Elements of X-ray Diffraction*, 2nd ed., Addison-Wesley, Reading, USA (1978).
21. R. Pérez-Casero, A. Gutiérrez-Llorente, O. Pons-Y-Moll, W. Seiler, R. M. Defourneau, D. Defourneau, E. Millon, J. Perrière, P. Goldner, and B. Viana, *J. Appl. Phys.* **97**, 054905 (2005).
22. M. Subramanian, P. Thakur, S. Gautam, K. H. Chae, M. Tanemura, T. Hihara, S. Vijayalakshmi, T. Soga, S. S. Kim, K. Asokan, and R. Jayavel, *J. Phys. D: Appl. Phys.* **42**,

105410 (2009).
23. Z. Sofiani, B. Derkowska, P. Dalasiński, M. Wojdyła, S. Dabos-Seignon, M. A. Lamrani, L. Dghoughi, W. Bała, M. Addou, and B. Sahraoui, *Opt. Commun.* **267**, 433 (2006).
24. H. J. Ko, T. Yao, Y. Chen, and S. K. Hong, *J. Appl. Phys.* **92**, 4354 (2002).
25. T. Koida, S. F. Chichibu, A. Uedono, A. Tsukazaki, M. Kawasaki, T. Sota, Y. Segawa, and Y. Koinuma, *Appl. Phys. Lett*. **82**, 532 (2003).
26. D. M. Hofmann, D. Pfisterer, J. Sann, B. K. Meyer, R. Tena-Zaera, V. Munoz-Sanjose, T. Frank, and G. Pensl, *Appl. Phys. A.* **88**, 147 (2007).
27. H. Ahn, Y. K. Young, C. K. Dong, S. K. Mohanta, and H. K. Cho, *J. Appl. Phys.* **105**, 013502 (2009).
28. R. Cusćo, E. Alarćon-Llado, J. Ibãnez, L. Arťus, J. Jimńez, B. Wang, and M. J. Callahan, *Phys. Rev. B* **75**, 165202 (2007).
29. R. Jothilakshmi, V. Ramakrishnan, R. Thangavel, J. Kumar, R. Saruac, and M. Kuball, *J. Raman Spectrosc*. **40**, 556 (2009).
30. J. Wrzesinski and D. Frohlich, *Phys. Rev. B* **56**, 13087 (1997).
31. M. Lucas, Z. L. Wang, and E. Riedo, *Phys. Rev. B* **81**, 04515 (2010).
32. V. Gupta, P. Bhattacharya, Y. I. Yuzuk, K. Sreenivas, and R. S. Katiyar, *J. Cryst. Growth* **287**, 39 (2006).
33. H. Liem, P. Etchegoin, and D. D. C. Bradley, *Phys. Rev. B* **64**, 144209 (2001).
34. S. Venkatesh, J. B. Franklin, M. P. Ryan, J. S. Lee, H. Ohldag, M. A. McLachlan, N. M. Alford, and I. S. Roqan, *J. Appl. Phys.* **117**, 013913 (2015).
35. X. Ma, *Thin Solid Films* **520**, 5752 (2012).